

UKIRT/WFCAM Survey Proposal

HiZELS: A WFCAM Survey for Emission Line Galaxies at $z=1-9$

Applicants

PIs: Ian Smail, Durham University, UK (ian.smail@durham.ac.uk)
Philip Best, Institute for Astronomy, Edinburgh, UK (pnb@roe.ac.uk)
Jim Geach, Durham University, UK
Kristen Coppin, Durham University, UK
Mark Casali, European Southern Observatory, Garching, Germany
Rob Ivison, Astronomy Technology Centre, Edinburgh, UK
Jaron Kurk, Max Planck Institute for Astrophysics, Heidelberg, Germany
Carlton Baugh, Durham University, UK
Cedric Lacey, Durham University, UK
Alastair Edge, Durham University, UK
Gavin Dalton, Oxford University, UK

Abstract

We propose a panoramic extragalactic survey utilizing a set of existing and custom-made narrow-band filters in the J, H and K-bands to detect emission line galaxies at $z=1-9$ across 10 sq. degrees. Our survey employs the H₂(S1) narrow-band filter to target H α emitting galaxies at $z=2.23$. In addition, in anticipation of this survey, we have purchased specially designed narrow-band filters targeting the [OII] 3727 and [OIII] 5007 lines at the same redshift as H α . These filters are currently mounted in WFCAM for observations in support of this proposal during 2006B. Together these three sets of filters will enable us to investigate the [OII] 3727, [OIII] 5007 and H α emission from galaxies at $z=2.23$, while the J- and H-band filters will deliver identically-selected H α samples at $z=0.84$ and 1.47 respectively. The comparisons between the luminosity function, the clustering and variation with environment of these H α -selected samples across $z=0.8-2.2$ will yield unique constraints on the evolution of star-forming galaxies. More speculatively, the J-band filter will be sensitive to Ly α emission from galaxies at $z=8.90$ and may detect a few such sources if current theoretical predictions are correct. To undertake this narrow-band survey we request an allocation of 103 nights over 5 years to map 10 sq. degrees.

1. Introduction

The key observables required to understand the basic features of galaxy formation and evolution are the volume-averaged star formation rate as a function of epoch, its distribution function within the galaxy population, and the variation with environment. Surveys of the star-formation rate as a function of epoch suggest that the star-formation rate density rises as $\sim(1+z)^4$ out to at least $z \sim 1$ (e.g. Lilly et al. 1996) indicating that most of the stars in galaxies today formed at $z \gtrsim 1$ and thus the “epoch” of galaxy formation occurs at $z > 1$. Determining the precise redshift where the star-formation rate peaked is more difficult, with different star-formation indicators giving widely different measures of the integrated star-formation rate density (see Smail et al. 2002). Nevertheless, there is a general trend for the star-formation rate density to flatten at $z \sim 2$ and thus it is likely that the bulk of stars seen in galaxies today were formed between $z \sim 1-3$. Indeed, $z \sim 2-2.5$ appears to be a critical era in the evolution of many populations such as QSOs and submillimetre galaxies, which may be intimately linked to the formation of massive galaxies (Boyle et al. 2000; Chapman et al. 2005).

Unfortunately, a detailed understanding of the evolution in the star-formation rate density is restricted by the inhomogeneous mix of star-formation rate indicators used to trace the evolution across these redshifts. These problems are exacerbated by the effects of cosmic variance in the current samples, which are typically based on small-field surveys. While no single indicator provides an unbiased view of the evolution of the star-formation rate density (Kewley et al. 2004), mixing different indicators at different epochs is not helping our understanding. What we require is a single star-formation indicator which can be applied from $z=0$ to $z \sim 3$, which is relatively immune to dust extinction and which has sufficient sensitivity that our estimate of the integrated star-formation rate doesn't require large extrapolations for faint sources below the sensitivity limit. $H\alpha$ luminosity is arguably the cleanest route to achieve these goals – it provides a very well-calibrated measurement of the star-formation rate (Kennicutt 1998; Moustakas et al. 2006), the emission line is relatively unaffected by moderate dust extinction and moreover it is bright enough that surveys with a sensitivity of $\sim 10 M_\odot \text{ yr}^{-1}$ can be undertaken at $z \sim 2$ with current instrumentation. This contrasts with the equivalent star formation rate limit at this epoch for other dust-independent tracers such radio, far-infrared or submillimetre surveys of $\sim 100-1,000 M_\odot \text{ yr}^{-1}$ (Ivison et al. 2006). The $H\alpha$ luminosity function (LF) for $H\alpha$ -selected galaxies (and their corresponding star-formation rate density) from spectroscopic and imaging surveys has been measured out to $z \sim 1.3$ by a series of investigators (Gallego et al. 1995; Yan et al. 1999; Glazebrook et al. 2004; Tresse et al. 2002; Doherty et al. 2006; Chun et al. 2006). These observations support the rapid rise seen by other star-formation indicators to $z \sim 1$ (Fig. 1), but few sensitive surveys have been undertaken at $z \sim 2$ (where redshifted $H\alpha$ begins to approach the thermal infrared) and those that have are hampered by small sample sizes (typically just ~ 10 sources, e.g. Moorwood et al. 2000).

How can we obtain $H\alpha$ -derived star-formation rates for large, robust and representative samples of galaxies at $z \gtrsim 1-2$, spanning the potential peak era of activity in galaxies and AGN?

Emission-line surveys are a particularly powerful method for tracing the evolution of star formation (and to a lesser extent AGN activity) as a function of cosmic epoch (Chun et al. 2006). With the advent of large-format imaging cameras in the optical and more recently in the near-infrared, we can exploit narrow-band filters to undertake sensitive and unbiased surveys for emission-line objects lying in well-defined large volumes across the relevant redshift range (out to $z \sim 2.5$), and potentially yielding thousands of sources. The main benefits of such surveys for studies of star formation are that the sources are identified on the strength of their emission line and thus crudely represent a star-formation rate-selected sample, and that they must lie in a narrow range in redshift. Hence, using a number of narrow-band filters it is possible to apply a single technique to target $H\alpha$ emitters across a wide range of redshifts, yielding large and representative samples at each epoch and with a uniform selection function. Such samples are ideal for tracing the evolution in the star-formation rate density

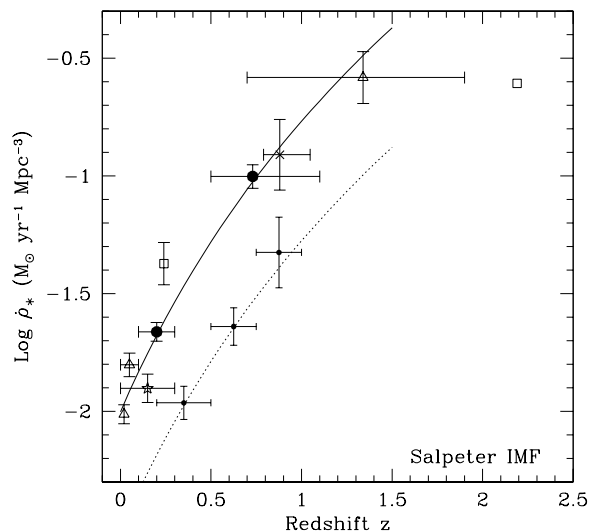


Fig. 1. The evolution of the star formation rate density as traced by current surveys of the $H\alpha$ (taken from Tresse et al. 2002). The figure shows the star formation density estimated from reddening-corrected $H\alpha$ observations (the point at $z \sim 2$ is from Moorwood et al. 2000) and three UV-observations from Lilly et al. (1996) [small diamonds]. The solid line is a fit of the form $(1+z)^{4.1}$, while the dotted line shows the same relation fit to the UV data points (which are systematically low). Our proposed survey will improve the reliability of the measurements at $z = 0.8-2.2$ by roughly two orders of magnitude.

across the era of peak activity in galaxies.

It is not only the global average star formation rate which is important for our understanding of galaxy formation and evolution, but more crucially the nature and distribution of the star forming galaxies at high redshifts. Many recent results point towards the star formation in the most massive galaxies occurring earlier than that in lower mass galaxies – so-called ‘down-sizing’ (e.g. Cowie et al. 1996; Bower & Balogh 2003), although the epoch of star formation of the most massive galaxies is currently poorly constrained. At low redshift, the star formation rates of galaxies are also greatly influenced by the environment in which they reside with star formation strongly suppressed in dense environments. To what extent is it the build-up of galaxies into groups and clusters since $z \sim 1$ that drives the decline in the cosmic star formation rate? This question can only be addressed by examining how the relationship between star-formation rate and environment evolves with redshift. Large $H\alpha$ surveys over the redshift range $z=0-2$ would provide a uniquely powerful tool for measuring the growing influence of environment on star-forming galaxies, and determine how the characteristic stellar mass of star forming galaxies changes with epoch. Such observations would yield key tests of current galaxy formation models (Benson et al. 2000; Baugh et al. 2005; Bower et al. 2006).

2. Our pilot narrow-band WFCAM Survey

Over the past year we have begun to exploit the unique capability of WFCAM for wide-field near-infrared narrow-band imaging. This pilot survey aimed to obtain a census of $H\alpha$ emitters at $z=2.23$ in two 0.75 sq. degree areas within the COSMOS and UKIDSS/UDS fields, and allows us to start to address two critical shortcomings of previous studies: small number statistics and cosmic variance (Fig. 2). WFCAM’s field of view is equivalent to ~ 30 Mpc at $z=2.23$ – allowing us to construct fair samples of hundreds of star forming galaxies at this redshift by mosaicing together a modest number of tiles. The data already analysed (in the COSMOS field) confirm that the survey is meeting expectations (Figs. 3). These observations have a $3\text{-}\sigma$ sensitivity of 1×10^{-16} ergs s^{-1} cm^{-2} , equivalent to a star-formation rate of $\sim 40 M_{\odot} \text{yr}^{-1}$. To a $5\text{-}\sigma$ flux limit we detect an integrated surface density of emission line objects of 280 ± 20 per sq. degree, in agreement with previous estimates based on $> 10 \times$ smaller areas ($\sim 360 \pm 110$, Moorwood et al. 2000). Our quoted error-bar is simply Poisson, but there is evidence that the emission-line selected sources are clustered across the frame, both on small and large scales. Work to confirm these sources as $H\alpha$ emitters through photometric redshifts and follow-up near-infrared spectroscopy with VLT is underway.

We have been allocated long-term status in Semester 2006B to extend our pilot survey in these two test fields to $H\alpha$ emitters at lower redshifts using new custom-made narrow-band filters in the J- and H-bands. These filters have been designed to correspond to the wavelengths of the redshifted [OII] 3727 and [OIII] 5007 emission lines at the same redshift as the $z=2.23$ $H\alpha$ -selected emitters, and they will also detect up to several hundred $H\alpha$ emitters at $z=0.84$ and 1.47 (see Table below). Combining the data at all three wavelengths, the survey will yield uniformly-selected samples of $H\alpha$ emitters at redshifts spanning the peak of the cosmic star formation. The completed pilot survey will represent at least an order of magnitude improvement in our understanding of emission-line selected $H\alpha$ samples at these redshifts. However, this pilot survey is still too small to reliably address the major questions raised earlier and so we are proposing here a further order-of-magnitude increase in the survey area.

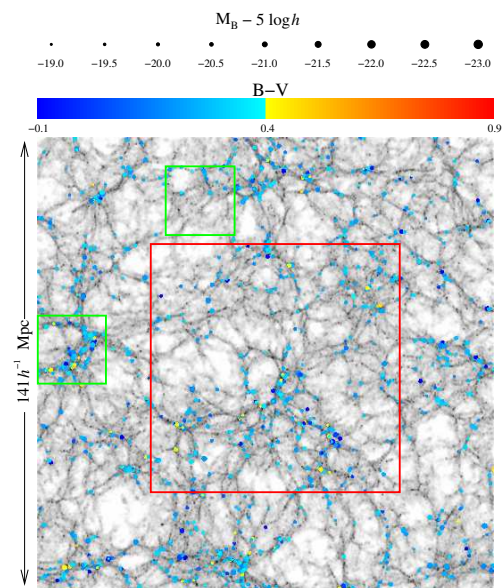


Fig. 2. A $\Delta z=0.03$ thick slice of the Universe at $z=2$, – identical to the volume probed by our narrow-band filters – from the GALFORM semi-analytic models of the Durham group (Benson et al. 2000). Galaxies are shown distributed on the underlying density field and are colour/size-coded on the basis of their luminosities and the colours of their stellar populations. These simulations illustrate the early formation of galaxies in the highest density regions which go on to form the passive cores of rich clusters at the present-day. The field of view of WFCAM is shown by the small boxes overlaid on the simulation – illustrating the likely cosmic variance even on this scale. The large box shows the proposed 10 sq. degree survey which provides a much fairer sample of the relevant clustering scales at this redshift (note that our area will not be contiguous and so will be less prone to any remaining cosmic variance issues).

λ (μm)	$z=8.90$	$z=2.23$	$z=1.47$	$z=0.84$
2.121	...	$H\alpha$
1.618	...	[OIII]5007	$H\alpha$...
1.204	$\text{Ly}\alpha$	[OII]3727	...	$H\alpha$

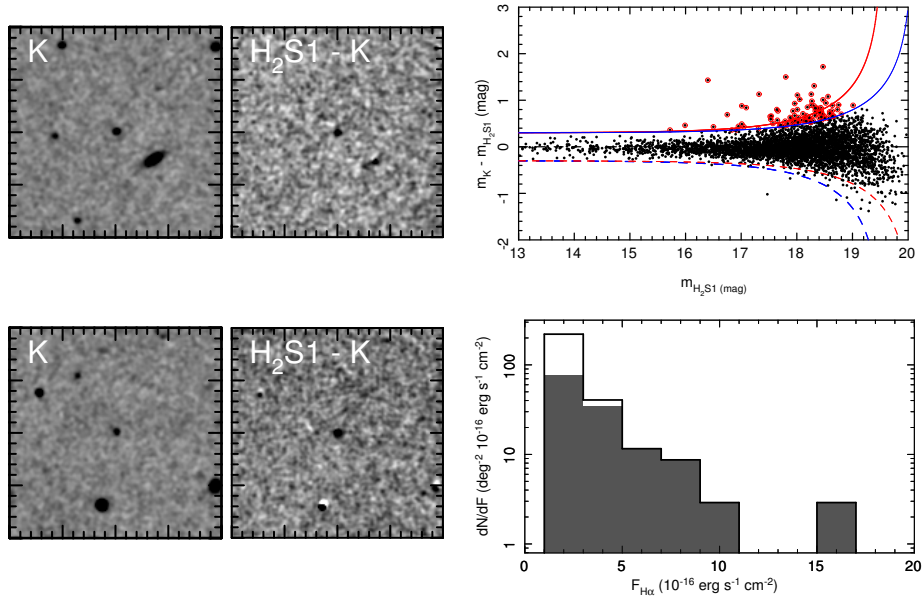


Fig. 3a. [left] Two examples of $z=2.2$ $H\alpha$ emitters taken from our pilot observations of the COSMOS field. The thumbnails show $1' \times 1'$ (0.5×0.5 Mpc) fields around the candidates. The comparison of broad-band (K) and continuum-corrected narrow-band (H_2S1) highlights the emission-line candidates in the centre of each panel. These data represent 5-hr exposures taken in typical conditions and it is clear that we are able to successfully select candidate narrow-band emission-line objects. We have approved VLT-ISAAC time to follow-up a sample of these emitters, which we will use to confirm the efficiency of our narrow-band selection technique. **Fig. 3b.** [upper-right] The colour-selection used to identify narrow-band excess objects: K– H_2S1 colours versus narrow-band magnitude. These data are taken from a ~ 0.2 -sq. degree region of the COSMOS field, with 18-ks integration in the narrow-band and 3.0-ks in K-band, identical to our proposed survey strategy, which yields a $3\text{-}\sigma$ sensitivity of 1×10^{-16} $\text{ergs s}^{-1} \text{cm}^{-2}$. This is consistent with expectations and sufficient to identify ~ 100 sources over this 0.21 deg^2 region above our $3\text{-}\sigma$ limit in agreement with the surface density estimated from other previous studies of much smaller areas (e.g. Moorwood et al. 2000). The curved lines show the 3 and $5\text{-}\sigma$ signal-to-noise limits and in addition we require an $\text{EW}(H\alpha) \geq 20\text{\AA}$. Circled points show the selection of these narrow-band excess objects (example thumbnails shown in the panel on the left). The small number of sources below the negative selection tracks demonstrate that we expect a low false-detection rate in our sample. **Fig. 3c.** [lower-right] Flux distribution of detected emitters at 3 - and $5\text{-}\sigma$ (outline and shaded respectively). Fluxes are calculated based on the narrow-band (H_2S1) excess over continuum.

3. This proposal

We propose to extend our three-filter narrow-band pilot survey of 1.5 sq. degrees to cover 10 sq. degrees of sky. The full survey will encompass star-forming galaxies in volumes of 1 , 2 and 3×10^6 Mpc^3 at $z=0.84$, 1.47 and 2.23 respectively. This extended survey will be carried out in the areas covered by the UKIDSS DXS survey, to take advantage of the complimentary multi-wavelength data available for those sky regions. The prime goal of these observations will be to investigate the evolution of the clustering of star forming galaxies across the peak epoch of cosmic star formation, and to determine how the luminosity function of star forming galaxies changes with both host galaxy properties and environment. We also propose to dedicate a small fraction of the time to pushing our $z=2.23$ $H\alpha$ survey to a sensitivity limit a factor of three deeper than the current observations, over one quarter of a WFCAM tile in each of the COSMOS and UKIDSS-UDS fields (i.e. approximately 0.4 sq. degrees in total). This will allow us to test the form of the faint end of the star formation LF at our highest redshift, and will provide a quality control check on the larger sample.

Our proposed survey will achieve the following scientific goals:

3.1 Trace evolution in the $H\alpha$ LF from $z=0.8$ – 2.2 .

We will determine the evolution of both the characteristic luminosity and the number density of $H\alpha$ emitters from $z=0.84$ to $z=2.23$. This survey will be the first to provide a fair sample of emission-line-selected galaxies at these epochs and the full survey will improve on the current published measurement of the star-formation rate at $z\sim 0.8$ – 2.2 by over two orders of magnitude. Our observations will yield a sample of a $4,000$ – $6,000$ galaxies at each epoch, allowing us to derive the LF in ten bins with (Poissonian) uncertainties in each bin of $< 5\%$ (c.f. Fig. 1). This will be sufficient not only to track the variation in the total $H\alpha$ luminosity density, but also to determine any strong changes in the shape of the LF. By integrating the $H\alpha$ LF we will obtain the first reliable estimate of the changes in the global star-formation rate of the Universe between $z=0.8$ and 2.2 using a single tracer of star formation. Combined with similar observations at lower redshifts (Chun et al. 2006), this

survey will track the $H\alpha$ LF from $z=0-2.2$.

The deeper $H_2(S1)$ observations in the COSMOS and UDS fields will enable us to probe the luminosity function at $z=2.23$ down to a depth more comparable to that achieved at the lower redshifts. Although the sky coverage will be much smaller, the use of two distinct fields will limit cosmic variance, and any residual bias can be estimated by comparing the number density of the more luminous $H\alpha$ emitters in these regions with the survey average. These deeper observations will also provide a quality-control check on the main sample, by providing nine distinct observations of the same fields each to the same depth as the main survey, thus enabling us to test both the reliability and the repeatability of detections close to the sensitivity threshold.

In the future, we can also stack the UV (from *GALEX*), radio (from eVLA) and submillimetre observations (from SCUBA-2) of our $H\alpha$ -selected catalogs to compare these tracers of the star-formation rate with $H\alpha$. This will allow us to investigate the apparent increase in the proportion of obscured star formation activity at higher redshifts (Dole et al. 2006), which is responsible for much of the far-infrared background.

To achieve these goals, it is necessary to identify which of the emission-line objects are indeed $H\alpha$ emitters. This step exploits the multiwavelength data in the UKIDSS DXS fields, backed up by statistical analysis of the contamination rates derived from follow-up spectroscopy of sub-samples of emitters with VLT, Gemini, UKIRT and most importantly FMOS on Subaru. Our survey targets $H\alpha$ emission-line sources at $z=0.84$, 1.47 and 2.23. Given the relative strength of emission lines in typical galaxies, it is expected that the other emission lines which will be detectable are $[OIII]5007$ and $[OII]3727$. By design, these lines fall into our narrow-band filters in J and H for a source at $z=2.23$. This will provide both a confirmation of the redshifts for a subset of the $H\alpha$ -selected sample and a route to remove sources with high $[OIII]5007/H\alpha$ ratios (indicative of AGN) from our census of the star formation at this epoch. However, we will also detect these lines from sources at other redshifts – with $[OIII]5007$ at $z=1.42$ falling into the J-band filter, $[OII]3727$ in the H-band at $z=3.35$ and $[OIII]5007$ in the K-band for sources at $z=3.23$. To remove this contamination we require information about the likely redshift of the emission-line source, but a comparison of the contamination redshifts for an individual filter shows that this does not have to be very precise: $\delta z/z \sim 1$. Sufficient precision can be obtained from the existing optical, near- and mid-infrared observations of these fields from the *Spitzer* SWIRE survey (IRAC 3.6–8 μ m), the UKIDSS DXS survey (J/K-bands) and the optical follow-up of that with Subaru (i-band). These fields are also covered by the Deep-wide component of the *GALEX* UV survey. Together these data will allow us to remove low-redshift star-forming contamination (seen by *GALEX*) and the iJHK+IRAC bands will track the 1.6 μ m bump (Sawicki 2002) over the relevant redshift range with sufficient precision to reject the contamination. We also note that Pan-STARRS will provide deep grizY imaging over these fields to improve the photometric redshift constraints if necessary, on a similar time-scale to this proposed survey (Durham and Edinburgh are both partners in Pan-STARRS).

3.2 Measure the clustering of the star forming galaxies

The proposed survey is also intended to give a robust measurement the clustering properties of the $H\alpha$ emitters, and the variation of the $H\alpha$ luminosity function with environment, across the peak epoch of star formation in the Universe. The correlation function for different galaxy populations provides important insights into their properties, including information about their relative masses and satellite populations. These observations provide a strong test of theoretical models of galaxy evolution and a direct input into these models. Hence it is this goal which primarily sets the size of the current survey.

To test our ability to measure the clustering amplitude of $H\alpha$ emitters in the proposed survey, we have constructed mock-catalogues based on redshift snapshots from the Durham semi-analytic code GALFORM (Benson et al. 2000; Baugh et al. 2005; Bower et al. 2006). The large simulation volumes allow us to match the proposed survey footprint, with a depth in redshift space equivalent to that sampled by the narrow-band filters at $z=0.84$, 1.47 and 2.23. These simulations provide not only the three-dimensional distribution of galaxies at the relevant redshifts, but also information about their current and past star formation activity (including apparent K-band magnitudes and $H\alpha$ fluxes). In this way we can accurately reproduce our sample selection, by matching the apparent number density of the brightest $H\alpha$ sources in the simulation slice at $z=2.2$ to our observed surface density (~ 300 per sq. degree, Fig. 3). We then use the same $H\alpha$ luminosity cut in the simulations outputs for $z=0.8$ and $z=1.5$ to identify the population we will sample at these epochs. We have repeated this analysis for two different galaxy formation recipes, those from Baugh et al. (2005) and Bower et al. (2006), to illustrate how our survey can be used to distinguish between current models. These differ in the details of the feedback mechanisms available to halt star formation (Bower et al. uses strong feedback from AGN in the most massive galaxies), the merger timescales for halos and the IMF in the resulting bursts.

We show results from the simulations in Fig. 4. We note first that the narrow-band selection removes almost all of the projection effects which usually degrade clustering analysis based on imaging data. The top panel in

Fig. 4 then illustrates that our current survey of two 0.75 sq. degree regions is insufficient to accurately measure the correlation function for $H\alpha$ emitters at $z=2.23$ (mostly due to cosmic variance between fields, see Fig. 2). In contrast our proposed 10 sq. degree survey should provide a fair estimate of the clustering strength of this population on scales from arcseconds to degrees. The wide range in scales probed by our contiguous fields will enable us to measure both the 1-halo and 2-halo contributions to the clustering.

The middle panel in Fig. 4 also demonstrates that a 10 sq. degree survey will be able to track the evolution of the clustering amplitude of star forming galaxies as the Universe doubled its age from $z=2.2$ to $z=0.8$. The clustering strength declines as expected as our survey traces more common, and thus less-biased, star forming galaxies at lower redshifts. The comparison of our survey results with the theoretical models will therefore give us a strong test of their predictions. This is illustrated in the bottom panel in Fig. 4 which contrasts the predicted clustering of $H\alpha$ emitters based on the Bower and Baugh galaxy formation recipes. These show a strong divergence in their clustering on small scales (the 1-halo term arising from satellites of a galaxy) underlining the usefulness of clustering as a test of the inputs adopted in galaxy formation models. In summary, our analysis of the $H\alpha$ mock catalogs indicates that our proposed survey should optimally cover an area of at least 10 sq. degrees to our adopted depth and will then provide a strong test of current galaxy formation models.

In addition to the statistical analysis of the clustering of the emission-line galaxies in the survey, we will also search for evidence of changes in the $H\alpha$ luminosity function with environment at each epoch. In the local Universe, star formation is suppressed in dense environments (e.g. Lewis et al. 2002; Gomez et al. 2003 Bower & Balogh 2003). Over what redshift $z \sim 0.8-2.2$ does this environmental influence begin to become important? Alternatively, if the suppression of SF is already in place in galaxy overdensities at $z=2.2$, then that would imply that galaxy evolution in such environments must be greatly accelerated over those in the field. By comparing the extent to which environment influences star formation rate as a function of epoch, we will test the hypothesis that it is largely the build-up of galaxies into groups and clusters that leads to the sharp decline in the global average star formation rate below $z=1$.

As we noted, the volume enclosed by the proposed survey is a few times 10^6 Mpc^3 at each redshift; the local space density of clusters with mass $M > 10^{15} M_\odot$ is approximately 1 per $3 \times 10^6 \text{ Mpc}^3$, so our 10 sq. degree survey is sufficient to give us one extremely massive structure at each epoch, and thus probe the full range of galaxy environments. Fig. 2 demonstrates the likely range in environment encompassed by our complete survey.

3.3 Determine the relation between SFR, host galaxy mass, and cosmic epoch

Galaxies form and evolve within the hierarchically growing dark-matter haloes of a Lambda-CDM Universe. The details of the galaxy formation process depend upon the complicated gas dynamics of star formation and feedback, and these processes are poorly understood. A surprising result of many recent studies is that the stellar populations of the most massive galaxies formed earlier than those of less massive galaxies – a process often referred to as downsizing, or anti-hierarchical growth. Massive galaxies must therefore form stars rapidly at an early epoch, and then have their star formation truncated, for example by feedback from AGN (e.g. Bower et al. 2006; Croton et al. 2006; Best et al. 2006). Determining the characteristic mass at which star formation begins to be truncated, as a function of cosmic epoch, would determine the physical processes involved in the downsizing activity and place tight constraints upon galaxy formation models.

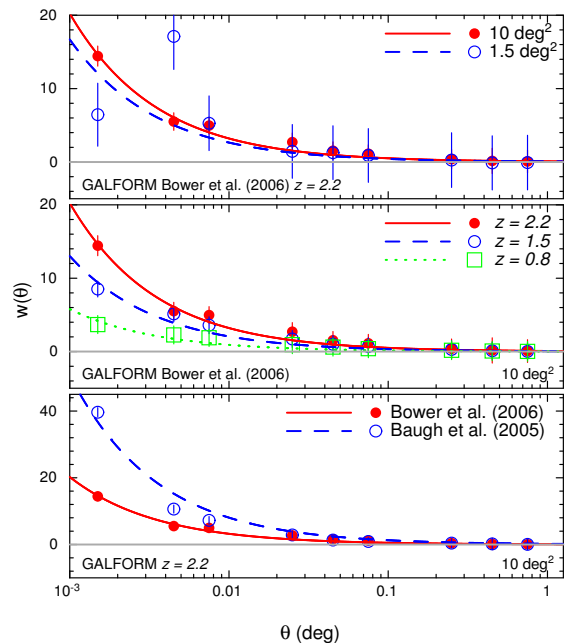


Figure 4a [top]. The variation as a function of area in the measured clustering of $H\alpha$ -selected galaxies at $z=2.23$ (matched to our observed surface density) selected from the latest GALFORM simulations (Bower et al. 2006). This demonstrates the improvement in the clustering measurements which we will obtain from expanding from our pilot survey of 1.5 sq. degrees to the full survey area of 10 sq. degrees. **4b [middle].** A comparison of the variation in the clustering strength of $H\alpha$ -selected galaxies in our three redshift slices based on the final survey area and depth. Again these predictions come from the GALFORM semi-analytic simulations in Bower et al. (2006) and they demonstrate that our survey will be able to reliably track the evolution in the clustering of star-forming galaxies across $z=0.8-2.2$. **4c [bottom].** Comparing the clustering of $H\alpha$ -selected galaxies at $z=2.2$ predicted by the recent Bower et al. (2006) galaxy formation model and that from Baugh et al. (2005). These two models differ in terms of the feedback and merger recipes they use – and it is clear from this plot that they predict very different clustering properties for the one-halo term (within $\sim 100 \text{ kpc}$ or ~ 0.01 degrees). As these various panels demonstrate, our proposed survey will provide a strong constraint on current models of galaxy formation and evolution.

As these various panels demonstrate, our proposed survey will provide a strong constraint on current models of galaxy formation and evolution.

To address this issue requires both stellar masses and star formation rates to be accurately determined across a wide range of redshifts. Combining our survey with low redshift surveys (Chun et al. 2006), we will determine robust star formation rates in an equivalent way for galaxies at least four epochs out to $z=2.2$. Stellar masses for all of these star forming galaxies will be determined from the deep near-infrared and optical imaging data available for our survey fields: at these redshifts, the accuracy of stellar mass estimates using multi-wavelength data from optical to $2.2\ \mu\text{m}$ is better than a factor of two (e.g. Drory et al. 2004). For the lower redshift samples, and the more massive galaxies at $z=2.2$, the addition of mid-infrared photometry from SWIRE will provide more accurate stellar mass determinations, and enable us to account for any systematics in the stellar mass estimates based on optical and near-infrared data alone. By combining these stellar masses with the star formation rates determined from the narrow-band surveys, we will determine how the characteristic stellar mass of $\text{H}\alpha$ -selected galaxy declines with redshift between $z=2.2$ and $z=0.8$.

On a three-year timescale, the addition of data in more optical wavelengths through Pan-STARRS and other surveys will enable us to also determine accurate photometric redshifts and stellar masses for the other galaxies in these regions, and therefore to determine how the mean star formation rate varies as a function of stellar mass at each epoch. These observations will provide a definitive measurement of the down-sizing effect, and a key test for models of galaxy formation.

The deeper observations in the $\text{H}_2(\text{S}1)$ narrow-band filter form an essential part of this project. They will enable us to sample down to the same star-formation rate at $z=2.2$ as we sample at $z=1.4$ ($\sim 10\ \text{M}_\odot\ \text{yr}^{-1}$); the comparable baseline between these two epochs will enable us to investigate any change in the characteristic mass of star forming galaxies as a function of star formation rate. These deeper observations will be undertaken in the survey regions with the optimal complimentary data (COSMOS and UDS).

3.4 Investigate the emission-line properties of the active population at $z=2.2$

The three narrow-band filters cover $[\text{OII}]\ 3727$, $[\text{OIII}]\ 5007$ and $\text{H}\alpha$ emission at $z=2.23$, to similar effective depths. By combining these datasets we will be able to identify AGN, as strong $[\text{OIII}]\ 5007/\text{H}\alpha$ emitters, and remove these from our census of star forming objects. We will also investigate these AGN separately, to study the environmental dependence of emission-line AGN activity at these high redshifts and compare this with the results from the SDSS and 2dFGRS surveys at low redshift (e.g. Miller et al. 2003; Kauffmann et al. 2004).

The survey will also identify star-forming galaxies at $z=2.23$ which have strong $[\text{OII}]\ 3727$ emission, but are relatively weak in $\text{H}\alpha$. Potentially, these might include lower-luminosity and lower-metallicity systems, allowing us to compare and contrast the clustering of high- and low-star-formation rate systems at $z=2.23$, to compare to results from SDSS at $z=0$. Finally, these data will identify dusty star-forming galaxies, with low $[\text{OII}]/\text{H}\alpha$ ratios, to similarly contrast their spatial distributions.

3.5 Search for $\text{Ly}\alpha$ at $z=8.90$

The most speculative, but potentially exciting, result from our expanded survey is the opportunity to identify very high- z sources through the presence of $\text{Ly}\alpha$ emission in our narrow-band J filter. This would correspond to $z=8.90$. Previous narrow-band $\text{Ly}\alpha$ searches have been extremely successful in detecting and confirming emitters (e.g. Hu et al. 2004, Venemans et al. 2006, Iye et al. 2006), including the detection of the most distant spectroscopically confirmed galaxy so far known ($z=6.96$). The discovery of $\text{Ly}\alpha$ emitters at $z\sim 9$, when the Universe was only ~ 0.5 Gyr old, would have important consequences for our understanding of the early star formation history of the Universe. How much star formation is on-going at this early epoch? Although extinction of the $\text{Ly}\alpha$ line will prohibit estimates of star formation rates based on its emission alone, the detection of objects at these redshifts will facilitate deep multi-wavelength follow-up observations, to investigate the star formation rate, existing stellar

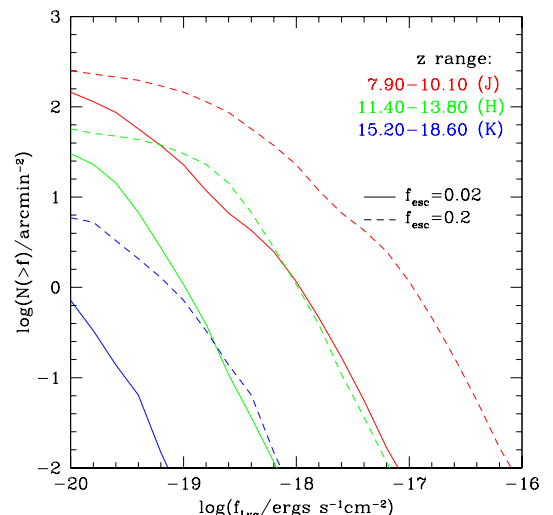


Fig. 5. A prediction of the $\text{Ly}\alpha$ LF from the Durham GALFORM code (taken from Le Delliou et al. 2005). This shows the predicted LF for three different redshift ranges, corresponding to the J (right-hand lines, relevant for our $z=8.90$ survey), H (middle lines) and K (left-hand lines) bands. It also shows LFs at each epoch for $\text{Ly}\alpha$ escape fractions of 0.2 and 0.02. Depending upon the escape fraction we could potentially detect several $z=8.90$ $\text{Ly}\alpha$ emitters in our survey. Predictions from Thommes & Meisenheimer (2005) are similar, suggesting several sources should be detected. However, the reader should note that a deep search for $\text{Ly}\alpha$ emitters at $z=8.8$ by Willis & Courbin (2005) with the VLT failed to detect any sources to a flux limit of $3 \times 10^{-18}\ \text{ergs cm}^{-2}\ \text{s}^{-1}$, suggesting escape fractions are likely to be < 0.2 , although these data cover only a very small field ($2.5'$ -square) and hence are extremely sensitive to cosmic variance.

mass content, and other properties of these early galaxies. This survey could therefore provide the first real insights into the earliest population of objects in the Universe.

$\text{Ly}\alpha$ emitters at $z \sim 9$ also provide an important probe of re-ionisation of the Universe: as the mean fraction of neutral hydrogen in the intergalactic medium increases, the $\text{Ly}\alpha$ emission will be strongly attenuated, leading to a change in the $\text{Ly}\alpha$ luminosity function. No significant evolution is seen in the $\text{Ly}\alpha$ luminosity function between $z = 5.7$ and $z = 6.5$, suggesting that the Universe is essentially fully ionised by $z = 6.5$ (Malhotra & Rhodes 2004) – although the details of this depend upon the level of local ionisation of the IGM by the star forming galaxies (Haiman & Cen 2005). Our survey could provide the first information about the $\text{Ly}\alpha$ luminosity function at $z = 9$, offering an important test of the epoch and process of reionisation.

A previous attempt to detect $\text{Ly}\alpha$ at $z = 9$ was unsuccessful (e.g. Willis & Courbin 2005), but only studied a sky area of $2.5'$ -square. Recent simulations of the expected number of $\text{Ly}\alpha$ emitters at this epoch (Le Delliou et al. 2005; see Fig. 5) indicate that for the most conservative assumptions ($\text{Ly}\alpha$ escape fractions of only 0.02), to the proposed depth of our survey we expect to detect perhaps one $\text{Ly}\alpha$ emitter across the entire 10 sq. degree survey. If the escape fraction is higher, we may detect tens of such galaxies. We note that this is the only element of our survey for which we know of direct competition – from a group (including ourselves!) using a similar J narrow-band filter on VISTA. We stress that this is the only narrow-band filter currently offered on VISTA and so narrow-band surveys of $\text{H}\alpha$ emitters at $z \geq 0.8$ are currently *only* feasible with WFCAM (WIRCAM and NEWFIRM have too small a field or available time on sky to undertake this proposed survey).

4. Summary

We request time to undertake a sensitive narrow-band survey over 10 sq. degree of the DXS regions, using the $\text{H}_2(\text{S}1)$ filter and custom-built narrow-band filters in the J and H bands. The survey will detect several thousand $\text{H}\alpha$ emitting galaxies at each of three redshifts (0.84, 1.47 and 2.23) spanning the likely peak in the star formation density of the Universe. This will be the first time that the luminosity function of star forming galaxies has been accurately determined at these epochs in a robust and uniform manner, and will pin-point the epoch when the star formation density of the Universe peaked. The angular cross-correlation function of the star forming galaxies, and its evolution with redshift, will be determined with sufficient accuracy to place tight constraints upon models of galaxy formation. The survey will also measure the growing influence of environment on star-forming galaxies, and any variations in the characteristic mass of the most active galaxies. It may also provide the first detection of the star forming galaxy at $z = 9$.

WFCAM is the first truly panoramic near-infrared imager, and it opens up entirely new discovery space in our understanding of high redshift galaxies. These narrow-band surveys will be un-paralleled in the foreseeable future, and will offer a lasting legacy.

References

- Baugh, C. M., et al., 2005, MNRAS, 356, 1191
 Best, P. N., et al., 2006, MNRAS, 368, L67
 Bower & Balogh 2003, astro-ph/0306342
 Chapman, S. C., et al., 2005, ApJ, 612, 2
 Cowie, L. L., et al., 1996, AJ, 112, 839
 Doherty, M., et al., 2006, MNRAS, 370, 331
 Drory, N., et al. 2004, ApJ, 608, 742
 Glazebrook, K., et al., 2004, AJ, 2652
 Haiman, Z., Cen, R., 2005, ApJ, 623, 627
 Ivison, R., et al., 2006, ApJ, in press (astro-ph/0607271)
 Kauffmann, G., et al., 2004, MNRAS, 353, 713
 Kewley, L. J., et al., 2004, AJ, 127, 2002
 Lewis et al., 2002, MNRAS, 334, 673
 Malhotra S., Rhodes J. E., 2004, ApJ, 617, L5
 Moorwood, A. F. M., et al., 2000, A&A, 362, 9
 Pahre & Djorgovski 1995 ApJ 449 L1
 Smail, I., et al., 2002, MNRAS, 331, 495
 Thommes & Meisenheimer 2005, A&A, 430, 877
 Venemans B., et al., 2006, A&A in press, astro-ph/0610567
 Yan, L., et al., 1999, ApJ, 519, L47
 Benson, A. J., et al., 2000, MNRAS, 331, 793
 Boyle, B. J., et al., 2000, MNRAS, 317, 1014
 Bower, R. G., et al., 2006, MNRAS, 370, 645
 Chun, L., et al., 2006, astro-ph/0610846
 Croton, D. et al., 2006, MNRAS, 365, 11
 Dole, H., et al., 2006, A&A, 451, 417
 Gallego, J., et al., 1995, ApJ, 475, 502
 Gómez, P., et al., 2003 ApJ, 584, 210
 Hu, E. M., et al. 2004, AJ, 127, 563
 Iye, M., et al., 2006, Nature, 443, 186
 Kennicutt, R., 1998, ARAA, 36, 189
 Le Delliou, M., et al., 2005, MNRAS, 357, L11
 Lilly, S. J., et al., 1995, ApJ, 455, L108
 Miller C.J., et al., 2003, ApJ, 597, 142
 Moustakas, J., et al., 2006, ApJ, 642, 775
 Sawicki, M., 2002, AJ, 124, 3050
 Tresse, L. et al., 2002, MNRAS, 337, 369
 Thompson, D. et al., 1996, AJ, 112, 1749
 Willis J. P., Courbin F., 2005, MNRAS, 357, 1348

5. Survey Strategy and Exposure Time Calculation

When designing our pilot survey we turned to previous work to assess the likely depth required for our science goals. Thompson et al. (1996) used 1–2 hr narrow-band K-band integrations with a poorly sampled camera (0.81"/pixel) on the 3.5-m Calar Alto telescope and detected a single confirmed emission-line source brighter than 3.5×10^{-16} ergs cm⁻² s⁻¹ in a total area of 276 sq. arcmin. A deeper, Keck survey by Pahre & Djorgovski (1995) reached a 3- σ limit 1×10^{-16} ergs cm⁻² s⁻¹, but only over a single 4 sq. arcmin field, detecting no sources in this small field. Moorwood et al. (2000) surveyed 100 sq. arcmin with the 3.5-m NTT to a typical depth of $\sim 10^{-16}$ ergs cm⁻² s⁻¹, detecting 10 sources above $\sim 3\text{-}\sigma$ (their coverage is highly non-uniform).

Our goal here is to match the depth of the sensitive Keck and NTT surveys, but over an area $> 100\times$ larger than the wide-field survey of Thompson et al. (1996). This combination should provide a sample of 1,000's of star-forming galaxies, sufficient to accurately define their luminosity function and clustering (see Fig. 4). We therefore aim for a 3- σ flux limit of 1×10^{-16} ergs cm⁻² s⁻¹ for our K-band narrow-band observations, which for H α at $z=2.23$ is equivalent to a star-formation rate of $40 M_{\odot} \text{ yr}^{-1}$ (in a WMAP cosmology). Using the WFCAM broadband sensitivities, and scaling by the width of the narrow-band filter, we estimated that this would take 18 ks in the H₂S1 filter and our pilot observations at this depth confirm this (Fig. 3). The pilot observations yield cumulative number densities of line emitters of 280 per sq. degree above 5- σ and 580 per sq. degree above 3- σ , which is consistent with the ~ 0.1 per sq. arcmin detected to this flux limit by Moorwood et al. (2000) and Yan et al. (1999). Given the success of the pilot study, we propose to continue with this strategy for the full survey. With 30% overheads, the 18ks per pixel exposure time translates into a total of 26 hrs to complete a filled WFCAM tile in the narrow-band. We also require continuum observations to compare to the narrow-band to identify line-emitters: these take approximately 1 hr per pixel – or 5 hrs for a complete tile with overheads. However, as we explain below, the continuum observations are only required in the H-band as we will be surveying regions with existing deep J/K-band observations from WFCAM (from UKIDSS DXS).

For the custom-filters in the J and H-band, we aim to reach at least the same emission line flux limits as in the H₂ S1 filter (1×10^{-16} ergs cm⁻² s⁻¹ at the 3- σ level) This will produce comparable H α surveys in terms of sensitivity and sample size (as the increased depth will compensate for the reduced volume of the survey at lower redshifts). Equally importantly, this choice maximises the information we can gather on the properties of the $z=2.23$ population from our matched [OII] 3727, [OIII] 5007 and H α surveys at this redshift. For example, a typical AGN will have [OIII]/H α ~ 1 so at $z=2.23$ we will be sensitive to bright AGN, and also identify star forming galaxies with unusually large [OII]/H α ratios (typical star forming galaxies have [OII]/H α ~ 0.6 ; Moustakas et al. 2006). This limit also provides a competitive sensitivity for the Ly α studies in the J-band narrow-band filter (Section 3.5 and Fig 5). We note that our 2006B narrow-band observations in the J-/H-band have not yet been undertaken and so we cannot yet confirm these sensitivity estimates from on-sky data.

For each WFCAM filled-tile our strategy requires a total exposure time of 26hrs each for the narrow-band observations in J, H and K and 5hrs in the continuum H-band observations, including 30% over-heads. Thus to survey a complete tile in all three filters will take 83 hrs. As explained in §3, our goal for area is to cover 10 sq. degrees, equivalent to 13 WFCAM filled-tiles, of which we will have two completed from the pilot project. The survey could be undertaken over a smaller region, but as shown in Fig. 4 this would yield poorer constraints on the clustering and LF. Hence, we base our time estimate on the goal of 10 sq. degrees – which will take 913 hrs to complete. In addition, we are requesting time to obtain data 3 \times deeper in the H₂(S1) filter on two single WFCAM-pointings (0.21 sq. degrees), in the COSMOS and UDS fields, to use to assess the reliability of our final sample. These observations require 52 hrs each (including overheads) for the narrow-band observations, along with matched K-band data in COSMOS (if this does not exist at the time), which will take 8 hrs. Suitable K-band data of course exists for the UDS. In total therefore we request 1025 hrs, or 103 nights, over five years.

Our aim is to place our survey patches within the DXS survey region. The DXS fields (Lockman Hole, XMM-LSS, SA22/VIMOS4 and ELAIS N1 regions) are the pre-eminent regions for multiwavelength surveys on $>$ degree scales, with coverage from the satellite UV (with GALEX) to the mid-infrared (from *Spitzer*) and in the near-future, far-infrared, submillimetre and radio. This combination of multiwavelength data will be combined with our volume-limited samples of emission-line selected galaxies at $z \sim 0.8\text{--}2.2$ to assess the variations in their obscuration, stellar masses, nuclear activity, etc. The DXS fields will also be the subject of FMOS follow-up where our survey will provide a powerful test sample of known strong emission-line sources. By pre-selecting galaxies with known emission lines in the J- and H-bands our survey provides ideal input for FMOS follow-up to gauge the kinematics of star forming galaxies and the dynamics of any structures they inhabit. Moreover, deep J/K broadband imaging already exists for 9 WFCAM tiles (in J/K) from the DXS survey, with more underway, thus reducing the time necessary for our observations. Because at least one DXS survey region is visible above an airmass of 1.5 for 90% of nights through-out the year, we can accept any scheduling, and our choice of fields within the DXS will be determined based upon observability on the allocated nights.

We can calibrate our deep narrow-band observations from shorter exposures (or the existing DXS continuum observations) and so do not require photometric conditions. Dark conditions are necessary for the J-narrow-band observations and grey conditions will improve our H-band sensitivity slightly. As typical $z = 0.84\text{--}8.90$ galaxies are likely to be compact we request $<0.8''$ seeing (we will use 2×2 microstepping).

6. Data Management Plan

We are anticipating that we will use the same pipelines and archiving as the standard UKIDSS data products, where relevant. Hence our data management will use the VISTA Data Flow System (VDFS) after the data frames are transported to the Cambridge Astronomical Survey Unit (CASU). Processed frames and per-frame catalogues will then be ingested into the WFCAM Science Archive (WSA) hosted by the Edinburgh Wide Field Astronomy Unit (WFAU). The final stages needed to produce survey products (Quality Control (QC) filtering, stacking, mosaicing, and band-merging) will be undertaken by our survey members at Durham and Edinburgh using large-memory workstations purchased for this purpose. We currently have three 4-processor machines each with 8–16 Gbs of memory and 2–4 Tb of direct storage, linked via gigabit Ethernet. These are in addition to the supercomputing resources available at both Durham and Edinburgh, to which we have access if required. All of the data shown in this proposal have been post-processed through our own pipeline in Durham.

Both the PI's hold Royal Society University Research Fellowships and we will have additional PDRA and PG effort available at Durham (1 PDRA and 1 PG) and Edinburgh (1 PG) over the survey lifetime to ensure timely planning, observing, reduction and analysis of the survey data. Further support will be requested in the rolling grant applications from our host institutions, and through fellowship applications, as the survey progresses. Based on the experience from our pilot survey, we believe this is sufficient effort to ensure we can produce and efficiently exploit the science data products from this survey (which requires only ~ 2 weeks observing per semester).

Contiguous sky-coverage over a WFCAM filled-tile is essential for our clustering analysis, and therefore our priority in carrying out the survey will be to complete tiles to the full depth, when started in a given filter. Individual tiles will be observed first in the K-band narrow-band filter, then in J- and H-band narrow-bands respectively. Our goal is to complete survey tiles in all 3 bands as soon as possible, in order to maintain equivalent areas at all three epochs. The deeper integrations in the COSMOS and UKIDSS-UDS fields will be spread over all 5 years, as scheduling permits.

Our aim is to release the survey data products in a staged manner as we finish their analysis. We anticipate that these releases will be made whenever a survey tile has been completed in all three narrow-bands. The precise timeline for these releases will therefore depend on the scheduling of our field coverage, which is flexible. However, a typical model might be: 2007/8/9/10/11B observations of XMM-LSS or SA22, 2008/9/10/11/12A observations of Lockman Hole and ELAIS N1, with publication of results and release of catalogues staggered by about 1 year.

We request the standard proprietary period (12 months) for these data.